Separation Science and Technology
Publication details, including instructions for authors and subscription information:
http://www.informaworld.com/smpp/title~content=t713708471

Modeling on the Counteractive Facilitated Transport of Co in Co-Ni Mixtures by Hollow-Fiber Supported Liquid Membrane

Jinki Jeong[a]; Jae-Chun Lee[a]; Wonbaek Kim[a]
[a] Minerals and Materials Processing Division, Korea Institute of Geoscience and Mineral Resources (KIGAM), Yuseong-Ku, Daejeon, Korea

Online publication date: 20 February 2003

To cite this Article Jeong, Jinki , Lee, Jae-Chun and Kim, Wonbaek(2003) 'Modeling on the Counteractive Facilitated Transport of Co in Co-Ni Mixtures by Hollow-Fiber Supported Liquid Membrane', Separation Science and Technology, 38: 3, 499 — 517
To link to this Article: DOI: 10.1081/SS-120016648
URL: http://dx.doi.org/10.1081/SS-120016648

MARCEL DEKKER, INC. • 270 MADISON AVENUE • NEW YORK, NY 10016

SEPARATION SCIENCE AND TECHNOLOGY
Vol. 38, No. 3, pp. 499–517, 2003

Modeling on the Counteractive Facilitated Transport of Co in Co–Ni Mixtures by Hollow-Fiber Supported Liquid Membrane

Jinki Jeong,* Jae-Chun Lee, and Wonbaek Kim

Minerals and Materials Processing Division, Korea Institute of Geoscience and Mineral Resources (KIGAM), Yuseong-Ku, Daejeon, Korea

ABSTRACT

The separation of cobalt from mixed solutions of cobalt and nickel sulfate through the hollow-fiber supported liquid membrane using 2-ethylhexyl-phosphonic acid mono-2 ethylhexyl ester as a carrier has been studied. A mathematical model was developed to analyze the permeation of cobalt in the competitive permeation of cobalt and nickel. The model was based on the continuity equation and considered not only the cotransport of cobalt and nickel, but also the counter-transport of hydrogen ions. The concentrations in the stripping solution were taken into account in the model as well as the concentrations in feed solution and liquid membrane. The experimental results were in good agreement with the model.

*Correspondence: Jinki Jeong, Minerals and Materials Processing Division, Korea Institute of Geoscience and Mineral Resources (KIGAM), 30 Gajeong-Dong, Yuseong-Ku, Daejeon 305-350, Korea; E-mail: jinki@kigam.re.kr.

DOI: 10.1081/SS-120016648 0149-6395 (Print); 1520-5754 (Online)

MARCEL DEKKER, INC. • 270 MADISON AVENUE • NEW YORK, NY 10016

Key Words: Model; Hollow fiber; Supported liquid membrane; Metal separation; Cobalt; Nickel.

INTRODUCTION

Development of a mathematical model is a necessity for the elucidation of supported liquid membrane (SLM) transport mechanisms. The model should be able to predict and optimize the practical separation processes using SLM. Even though the hollow-fiber supported liquid membrane (HFSLM) is expected to be one of the most promising candidates for future commercial applications, there have been only few attempts to model the system. In earlier studies, the models were analyzed by the stagnant-film theory which was applied for flat-sheets SLM (FTSLM) considering simply the shape as a cylinder.[1–3]

However, the film theory applies only to the case of turbulent flow. Since the nature of hollow-fiber modules does not allow turbulent flow of the feed or the strip solutions and the resultant flow is laminar, the film theory should not be applied to this case. Therefore, a model was suggested to analyze the system by the continuity mass-conservation equation, including the flow and the diffusion inside the fiber wall.[4,5] In most cases the same governing equation and system are used, but the analytical method and model are determined by the boundary conditions. Among the boundary conditions, the calculation of concentration at the interface is the most important parameter in this system. Generally, the boundary conditions were simplified, comprising several parameters to solve the system as a whole.

Kim et al.[4] performed a mathematical modeling by transforming a partial differential equation to an ordinary differential equation using a symmetrical orthogonal-collocation method. The concentration gradient was defined as the concentration difference between the feed and strip solution. The boundary conditions were further simplified by introducing facilitated coefficient and countertransfer coefficient. Urtiaga et al.[5] has analyzed the concentration at the interface by Leveque's approximation solution, assuming that the concentration at the wall is uniform when the mass transport is high in a short fiber.

None of the previous models considered the diffusion resistance of hydrogen ions at the interface between the feed solution and liquid membrane.[1–5] In most cases, the diffusion resistance of hydrogen ions was ignored since the size of a hydrogen ion is much smaller than that of metal ions. The diffusion resistance for hydrogen ions should, however, be included to extend the applicability of the model to high metal-concentration regimes. Generally, the conditions of strip side were not taken into account except for

few studies where the simple reaction of complex formation was used. This is because the concentration of hydrogen ions is high in the strip solution, and thus, the transport of metal ions is not affected by the conditions in the strip solution. However, since excessive supply of hydrogen ions results in unnecessary cost, it is favorable to determine the optimum hydrogen-ion ranges.

In this study, a mathematical model was developed for the permeation of cobalt from mixed solutions of cobalt and nickel sulfate through the HFSLM using 2-ethylhexylphosphonic acid mono-2 ethylhexyl ester [HEH(EHP)] as a carrier. The model includes the countertransport of hydrogen ions. The conditions of the stripping solution were considered in the model as well as the conditions of the feed solutions. In this model, the concentrations at the interface calculated from the concentration gradient of the carrier and metal ions in the liquid membrane were compared with those calculated from the permeation rate at the interface between the feed solution and the liquid membrane. The procedure was repeated to obtain the concentrations at the interface, which satisfies all constituents in the system. To complete the mathematical description of the model, the governing equation was expressed in finite difference form. As an independent variable has open ranges, this equation was solved using step-by-step methods for initial value problems.[6]

MODELING OF HOLLOW-FIBER SUPPORTED MEMBRANE

The steps that characterize the transport of cobalt and nickel through the liquid membrane are described as follows:[1,7,8]

- The free metallic species, after being transported to the interface between the feed solution and the liquid membrane, react with the carrier.
- The metal–carrier complexes diffuse through the organic phase of the liquid membrane.
- At the interface between the liquid membrane and the stripping solution, the metal–carrier complex liberates the metal ions to the aqueous phase, exchanging them for hydrogen ions.
- The uncomplexed carrier travels back through the liquid membrane.

To formulate the model, the following assumptions were made:

- The feed and strip solutions are Newtonian fluid.
- The feed solution enters the membrane lumens in fully developed laminar flow.[9,10]

- The concentration profile of feed solution in the lumens is developing.[9,10]
- Axial diffusion is negligible compared to axial convection. [This assumption is valid when the Peclet number is greater than 100[11]].
- The metal species diffuse in the organic medium only as metal–carrier complex.
- Cobalt and nickel ions do not interfere with each other in transport.
- The formation of complex at the interface is a parallel reaction for cobalt and nickel.
- The solubility of the carrier in the aqueous phase is negligible, and thus, its concentration in the membrane remains constant.
- Chemical reactions between the metal species and the carrier are instantaneous.
- The counterdiffusion of the free carrier in the membrane is not rate-determining and is ignored in the steady-state membrane flux.
- The reaction for complex formation at the interface is described as follows by Komasawa,[12] Preston,[13] and Newman et al.:[14]

$$Co^{2+} + 2\overline{(HR)_2} \Leftrightarrow \overline{CoR_2(HR)_2} + 2H^+$$

$$Ni^{2+} + 3\overline{(HR)_2} \Leftrightarrow \overline{NiR_2(HR)_4} + 2H^+$$

where $(HR)_2$ represents the HEH(EHP) dimer.

Commercial hollow-fiber devices normally contain a bundle of many hollow fibers. It is assumed that the conditions in a single fiber are identical and independent of each other. Figure 1 shows a schematic drawing of the single hollow-fiber system.

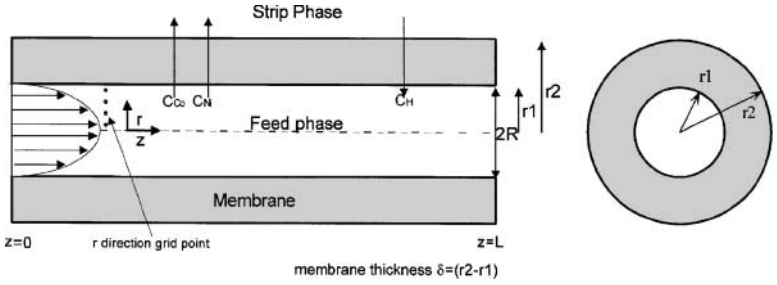

Figure 1. Schematic drawing of a single hollow fiber with counteractive facilitated-transport mechanism.

At steady state, the mass-conservation equation and the associated boundary conditions are given by[15,16]

$$\frac{\partial C}{\partial Z} = D/(2v_0[1-(r/R)^2])(\frac{1}{r}\frac{\partial C}{\partial r} + \frac{\partial^2 C}{\partial r^2}) \tag{1}$$

B.C. 1;

$$[\mathrm{Co}]_\mathrm{F} = [\mathrm{Co}]_{\mathrm{F,in}},\ \ [\mathrm{Ni}]_\mathrm{F} = [\mathrm{Ni}]_{\mathrm{F,in}},\ \ [\mathrm{H}]_\mathrm{F} = [\mathrm{H}]_{\mathrm{F,in}} \quad \text{at z} = 0,\ \text{all r} \tag{2}$$

B.C. 2;

$$\frac{\partial [Co]_F}{\partial r} = \frac{\partial [Ni]_F}{\partial r} = \frac{\partial [H]_F}{\partial r} = 0 \quad \text{at r} = 0, \quad \text{all z} \tag{3}$$

B.C. 3. at r = r1, all z

$$-D_{Co}\frac{dC_{Co,F}}{dr_{r=r1}} = k_{Co}\cdot s\cdot([\overline{CoR_2(HR)_2}]_{F,i} - [\overline{CoR_2(HR)_2}]_{S,i}) \tag{4}$$

$$-D_{Co}\frac{dC_{Ni,F}}{dr_{r=r1}} = k_{Ni}\cdot s\cdot([\overline{NiR_2(HR)_4}]_{F,i} - [\overline{NiR_2(HR)_4}]_{S,i}) \tag{5}$$

$$-D_{H}\frac{dC_{H,F}}{dr_{r=r1}} = k_{H}\cdot s\cdot([\overline{(HR)_2}]_{F,i} - [\overline{(HR)_2}]_{S,i}) \tag{6}$$

where subscript F represents feed; S, strip; i, interface; and in, initial. S is shape factor and expressed as s = [r2 − r1)/(r1*log(r2/r1)] (4). k is the mass-transfer coefficient in the membrane and written as $k = De/(\mathrm{r2} - \mathrm{r1})$.

The supplementary equations for the calculation of concentrations of cobalt, nickel, and hydrogen ions satisfying boundary condition 3 are:

S.E. 1. The interfacial reaction is so fast that the local chemical equilibrium is maintained. The equilibrium relationships at both interface of the membrane are given as:

$$[\overline{CoR_2(HR)_2}]_{F,i} = \frac{K_{Co}\cdot[Co]_{F,i}\cdot[\overline{(HR)_2}]^2_{F,i}}{[H]^2_{F,i}} \quad \text{at r = r1} \tag{7}$$

$$[\overline{NiR_2(HR)_4}]_{F,i} = \frac{K_{Ni}\cdot[Ni]_{F,i}\cdot[\overline{(HR)_2}]^3_{F,i}}{[H]^2_{F,i}} \quad \text{at r = r1} \tag{8}$$

$$[\overline{CoR_2(HR)_2}]_{S,i} = \frac{K_{Co}\cdot[Co]_{S,i}\cdot[\overline{(HR)_2}]^2_{S,i}}{[H]^2_{F,i}} \quad \text{at r = r2} \tag{9}$$

$$[\overline{NiR_2(HR)_4}]_{S,i} = \frac{K_{Ni}\cdot[Ni]_{S,i}\cdot[\overline{(HR)_2}]^3_{S,i}}{[H]^2_{S,i}} \quad \text{at r = r2} \tag{10}$$

S.E. 2. Mutual relationship between metal–carrier complexes in liquid membrane is expressed as follows:

$$k_{HR}([\overline{(HR)_2}]_{S,i} - [\overline{(HR)_2}]_{F,i}) = 2k_{Co}\cdot[\overline{CoR_2(HR)_2}]_{F,i} + 3k_{Ni}\cdot[\overline{NiR_2(HR)_4}]_{F,i} \tag{11}$$

S.E. 3. Total concentration of the carrier is conserved because the dissolution of carrier in the aqueous phase is negligible.

$$[\overline{(HR)_2}]_{in} = \frac{\int_{r1}^{r2} 2\pi r([\overline{(HR)_2}] + 2[\overline{CoR_2(HR)_2}] + 3[\overline{NiR_2(HR)_4}])dr}{\int_{r1}^{r2} 2\pi r\, dr} \tag{12}$$

where $[HR]_{in}$: initial concentration of carrier

To our knowledge an analytical solution to Eqs. (1)–(6) is not available since the third boundary condition is coupled with Eqs. (7)–(10) and nonlinear. Instead, we adopted a finite difference scheme using a step-by-step method for the initial value problem.[6]

EXPERIMENTAL

PC88A from Daihachi Chemical Industry Co. was used as a carrier without further purification. Commercial EP grade kerosene from Junsei Chemical Co. was used as diluent. The hollow-fiber module was made by Hoechst Celanese Co. The specifications of the liquid membrane supporter are: Liqui-Cel; polypropylene; 3600 fibers; fiber length, 16 cm; fiber I.D., 24 μm^2, total surface area, 0.4 m^2; fiber-wall thickness, 30 μm; porosity, 30%. The HFSLM was prepared by flowing the organic solution through the tube side of fibers and soaking the microporous fiber walls for at least 30 min. The liquid membrane solutions were prepared by diluting the carrier in the kerosene at a predetermined weight ratio. The cobalt and nickel sulfate solutions were used as feed solution after adjusting acidity by adding NaOH or H_2SO_4. The stripping solution was 3N sulfuric acid throughout the experiment.

The feed and stripping solutions passed through the tube side and shell side of fibers, respectively. The concentrations of metal ions in the aqueous phase were measured by the inductively coupled plasma-atomic emission spectrometry (ICP-AES, JOBIN YVON, JY 38+). The schematic diagram for the separation of cobalt and nickel ions by HFSLMs is presented in our previous study.[22]

RESULTS AND DISCUSSION

Determination of Parameters for the Model

Since mass transfer in a hollow fiber occurs only by diffusion due to laminar flow, the diffusion coefficient is required to calculate the concentration of metal ions at the interface. The diffusivity of cobalt ion and nickel ion obtained by Danesi et al.[17] was used in the calculation. The diffusivity of a free hydrogen ion was calculated using the Nernst–Haskell equation.[18,19] This value was similar to that obtained by adjusting the diffusivity of the hydrogen ion of hydrochloric acid in water to the diffusivity of sulfuric acid with the heavier molecules.[19]

The extraction equilibrium constant of cobalt (K_{Co}) and nickel (K_{Ni}) by HEH(EHP) was cited from the experimental results of Komasawa et al.[12] The effective diffusivity of the cobalt–carrier complex in the membrane phase (De_{Co}) was determined by adjusting the model to the permeation rates, which was obtained in experiments conducted as a function of pH, flow rate, and concentration of cobalt and nickel in the feed solution.

The Wilke–Chang equation, which is well known for its usefulness in the calculation of diffusivity, is reported to exhibit large deviations for organic solvents.[20] Therefore, the Stokes–Einstein equation, which is known to be more suitable for the diffusion of heavier molecules, was used instead.[16] The effective diffusivity of the nickel–carrier complex in the membrane phase (De_{Ni}) was estimated by applying the Stokes–Einstein equation to that of the cobalt–carrier complex in the membrane phase (De_{Co}).

The parameters used for the model calculations are listed in Table 1.

Evaluation of the Model

Figures 2, 3, and 4 show the comparison of permeation rates obtained in experiments and model prediction. It is believed that the deviation might be

Table 1. Parameters used for the HFSLM model calculation.

D_{Co}	6.9×10^{-10}	(m^2/s)	D_{Ni}	6.9×10^{-10}	(m^2/s)
De_{Co}	6.0×10^{-13}	(m^2/s)	De_{Ni}	4.8×10^{-13}	(m^2/s)
K_{Co}	3.4×10^{-6}	(—)	K_{Ni}	2.4×10^{-10}	(m^3/mole)
D_H	2.6×10^{-9}	(m^2/s)	δ	3.0×10^{-5}	(m)

due to the lack of ionic interactions between cobalt, nickel, and carrier in the model.

Figure 2 shows the effect of the metal ions in the feed solution on the competitive permeation of cobalt. The model is likely to slightly underpredict the permeation of cobalt at high metal concentrations, but the prediction for cobalt is in a fair coincidence with experimental data as can be seen from the coefficient of determination (r^2) of 0.930. Since the extractabilities of cobalt and nickel from the multicomponent solution are greater than those from the single-component solution due to the increase in the ionic strength of feed

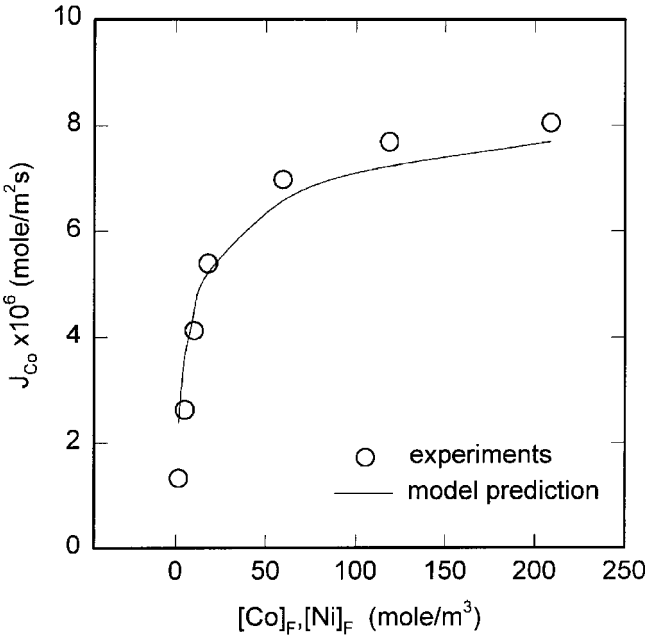

Figure 2. Changes in Co permeation rates with $[Co^{+2}]_F$ and $[Ni^{+2}]_F$ in HFSLM (pH = 4.7, flow rate = 1000 ml/min, carrier = 10 wt.%).

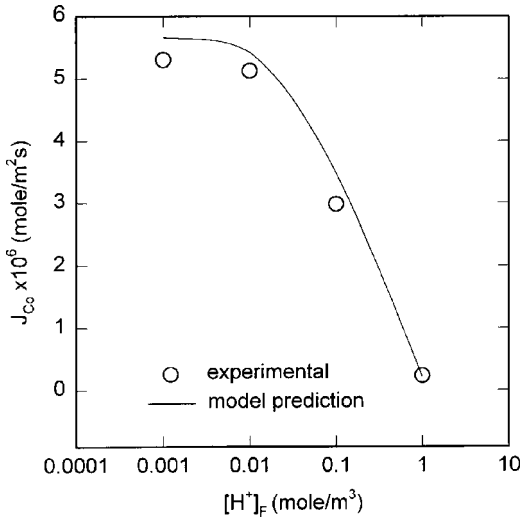

Figure 3. Changes in Co permeation rates with $[H^+]_F$ in HFSLM ($[Co^{+2}]_F$, $[Ni^{+2}]_F = 17\,mol/m^3$, carrier = 10 wt.%, flow rate = 1000 ml/min).

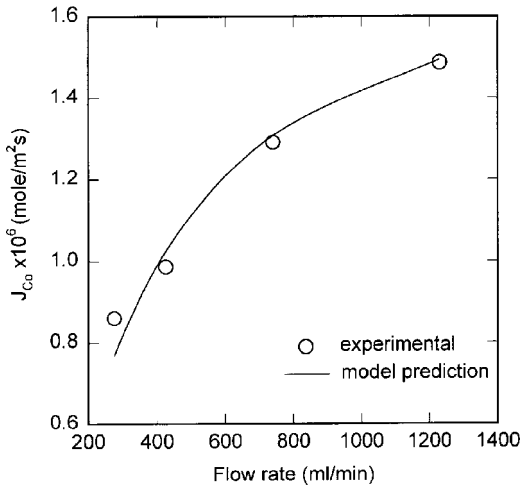

Figure 4. Changes in Co permeation rates with flow rate in HFSLM ($[Co^{+2}]_F = 0.85$, $[Ni^{+2}]_F = 85\,mol/m^3$, $pH_F = 6$, carrier = 30 wt.%).

solution, the permeation rates obtained by experiments were higher than those of model prediction.[12] The other reason for the underprediction might be the aggregation of the metal–HEH(EHP) complexes, which enhances the permeation for high metal concentrations.[14,21,23]

The effect of the bulk hydrogen concentration in the feed solution on the permeation rate of cobalt is shown in Fig. 3. The coefficient of determination is 0.973. At concentration higher than 0.01 mole/m^3, the permeation rate of cobalt increases sharply with the decrease of the hydrogen ion because the formation of the cobalt–carrier complex at the interface between the feed and liquid membrane is favored according to the equilibrium relationship. However, when the hydrogen concentration decreases below about 0.01 mole/m^3, it is seen that the permeation rate is limited and the effect of the hydrogen was negligible. This limitation can easily be understood considering the saturation of carrier at the interface between the feed solution and liquid membrane. In a real system, concentrations lower than 0.001 mole/m^3 is not a good operation condition because cobalt and nickel hydroxide precipitates begin to form.

Figure 4 shows the effect of flow rate in the feed solution on the permeation rates of cobalt. It is shown that the permeation rate estimated by the model is in good agreement, showing coefficient of determination of 0.957. The permeation rate of cobalt increases sharply with the increase of the flow rate in the feed solution.

Simulation

The concentration profiles of cobalt in lumen of HF were shown in Figures 5 and 6. It suggests that changes in flow rate affect the concentration distribution at exit side of the feed solution. Since the flow of the feed solution is lamina, changes in concentration of cobalt at the interface are not significant, as shown in Figure 6. At low flow rate, the concentration of cobalt decreases from the center towards the interface between the feed solution and liquid membrane. This is because cobalt ions are depleted as they transfer from the feed solution to the liquid membrane. Meanwhile, the concentration gradient between the bulk solution and the interface is reduced by instantaneous compensation of cobalt by the increase in the flow rate. It was shown that, in short fibers such as HF, the concentration profile becomes more pronounced as the flow rate decreases. Therefore, the fast flow that decreases the development of concentration profile is required to enhance mass-transfer efficiency.

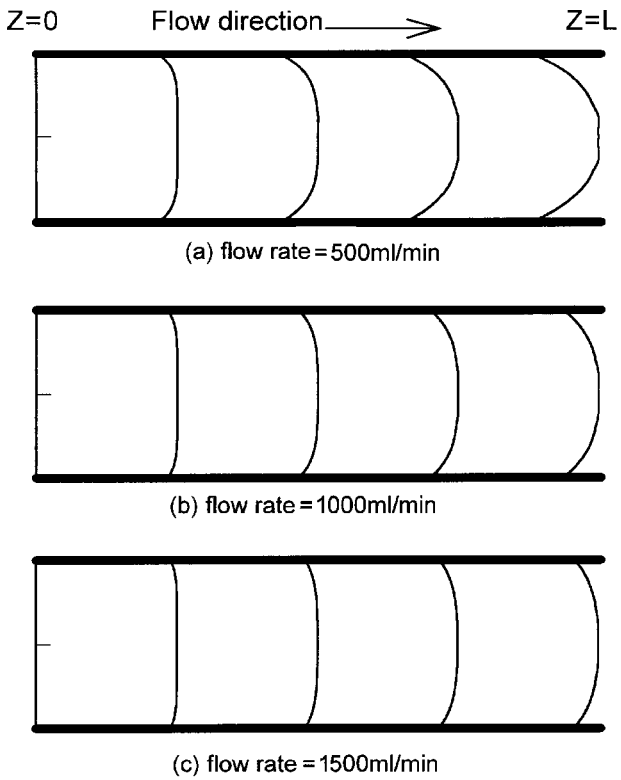

Figure 5. Concentration profiles of Co in the tube side of HFSLM at various flow rates.

Figure 7 shows the permeation rate and separation factor of cobalt with the carrier composition. The separation factor is defined as follows.

$$\text{Separation factor} = \frac{J_{Co}/[Co^{+2}]_{F,in}}{J_{Ni}/[Ni^{+2}]_{F,in}}$$

The permeation rate increases with carrier concentration, showing a maximum, and decreases rather rapidly afterwards. The maximum was shown at carrier concentrations of about 50–60 wt.%. This result agrees with the data of Youn et al. using FTSLM.[21] The permeation rate increases since cobalt–carrier complexes are formed more at the interface between the feed solution and liquid membrane with the increment of carrier concentration. At the same time, the increase in carrier concentration increases the viscosity of the liquid

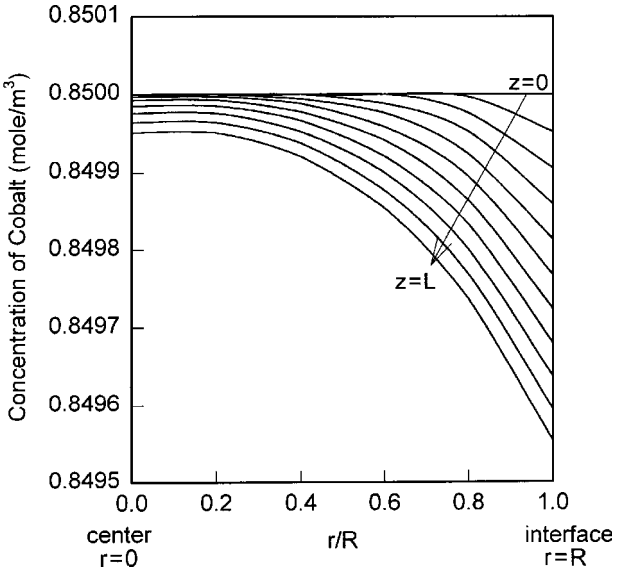

Figure 6. Concentration profiles of Co in the feed phase ($[Co^{+2}]_F$, $[Ni^{+2}]_F = 0.85\,mol/m^3$, $pH_F = 6.0$, carrier = 10 wt.%, flow rate = 280 ml/min).

membrane. This effect retards the diffusion of cobalt–carrier complexes in liquid membrane and consequently reduces the permeation rate of cobalt. According to the Stokes–Einstein equation, the diffusivity is inversely proportional to the viscosity.[19] The viscosity of HEH(EHP) used as a carrier increases with its concentration, especially at over 50 wt.%. The complex formation increases slightly with concentration but the effective diffusion coefficient decreases rapidly, resulting in the maximum at about 50–60 wt.%. As a consequence, the rate of complex formation increases with concentration upto about 50 wt.%, but the effective diffusivity decreases rapidly, showing the permeation rate maximum at 50–60%. With the increase in carrier, the separation factor of cobalt continues to decrease. As previously stated, the cobalt–carrier complexes at the interface increase with carrier concentration. However, the nickel–carrier complexes at interface increase at the same time, resulting in the decrease of the separation factor as observed. At concentrations over 50 wt.%, the separation factor of cobalt does not decrease further, despite the strong reduction in the permeation rate of cobalt. This is because the increase in the viscosity of the liquid membrane by the increase in the carrier concentration limits the permeation of nickel as well as that of cobalt.

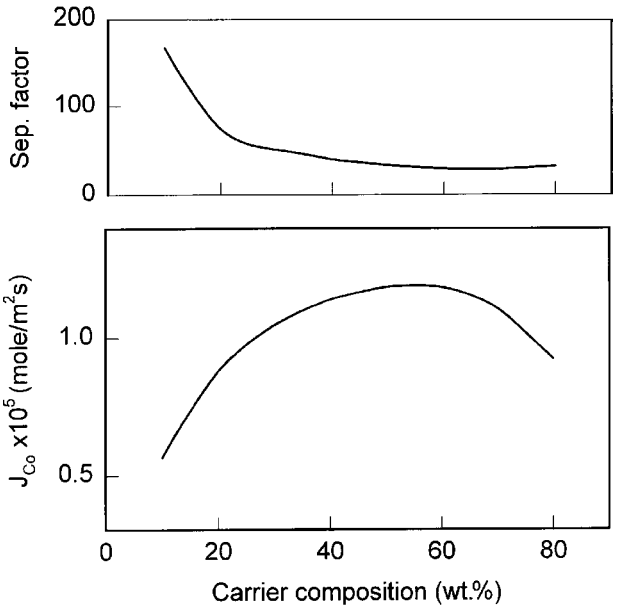

Figure 7. Effect of carrier composition on the permeation rate and separation factor of Co ($[Co^{+2}]_F$, $[Ni^{+2}]_F = 17\,mol/m^3$, $pH_F = 6.0$, carrier = 10 wt.%, feed flow rate = 1000 ml/min).

The permeation rate of cobalt at various flow rates of the feed solution and carrier concentration is shown in Figure 8. The permeation rate of cobalt becomes higher as flow rate increases. At above 500 ml/min of the flow rate, the permeation becomes constant. The permeation rate increases since the increase of flow rate reduces the mass-transfer resistance in the feed solution. But the permeation rate of cobalt is determined by the mass-transfer coefficient in the liquid membrane at higher flow rate where mass transfer coefficient in the feed solution is much higher than that in the liquid membrane.

The effect of flow rate of the feed solution and carrier concentration on the separation factor is shown in Figure 9. At low flow rate, the mass-transfer coefficient in the feed solution is more important to the controlling step of the cobalt permeation than that in the liquid membrane. Therefore, the increase in the flow rate results in the increase of cobalt permeation and, consequently, in the separation factor. When the flow rate becomes higher than a critical value, the mass-transfer coefficient in the feed solution is no longer the controlling step of the cobalt permeation. Instead, the role of mass-transfer

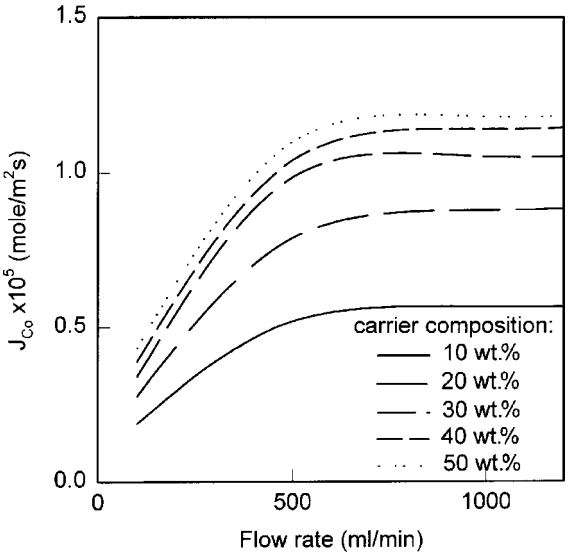

Figure 8. Effect of flow rate on Co permeation rate at various carrier compositions ($[Co^{+2}]_F$, $[Ni^{+2}]_F = 17\ mol/m^3$, $pH_F = 6.0$).

coefficient in the membrane becomes important, making the separation factor constant as observed.

Figure 10 shows the variation of metal concentration in feed solution and strip solution tanks with time. The conditions used were: volume of feed and strip solution, 1.25 L; carrier concentration, 10%; and initial cobalt and nickel concentration in feed solution, 17 mol/m^3. The permeation rates are observed to depend on changes in experimental parameters such as flow rate, initial concentration of metal ions, carrier concentration, and hydrogen-ion concentration in the feed solution. The rate of decrease in the concentration in feed solution reduces with time. The active facilitated transport, in which concentration in feed solution becomes higher than that in strip solution, can be seen after 80 min in the figure. As time increases, cobalt ions are depleted in the feed solution. The depletion of cobalt induces the formation of nickel–carrier complexes, resulting in the increase of the nickel concentration in strip solution. Therefore, the permeation time should be determined considering the recovery rate and purity of cobalt recovered.

Figure 11 shows the effect of operation time on the recovery and cumulative selectivity (separation factor) of cobalt at various carrier

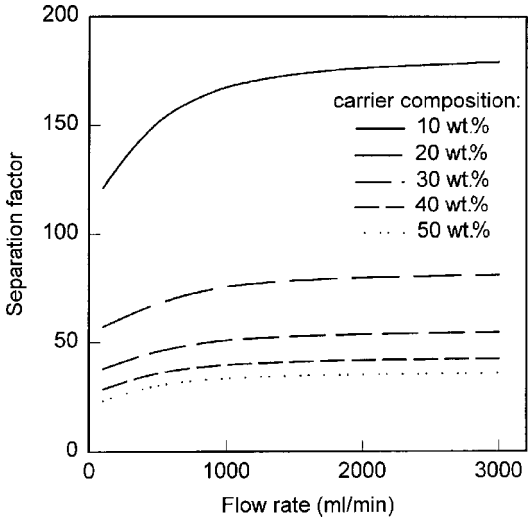

Figure 9. Effect of flow rate on the separation factor of Co at various carrier compositions ($[Co^{+2}]_F$, $[Ni^{+2}]_F = 17\,mol/m^3$, $pH_F = 6.0$).

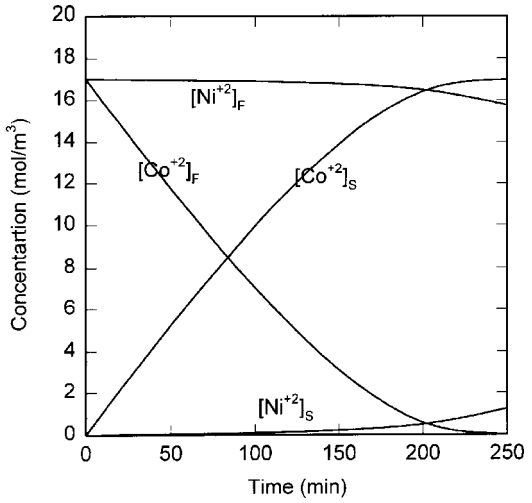

Figure 10. Simulation for the enrichment of Co with time ($[Co^{+2}]_F$, $[Ni^{+2}]_F = 17\,mol/m^3$, $pH_F = 6.0$, carrier = 10 wt.%, feed flow rate = 1000 ml/min, feed and receiving volume = 1250 ml).

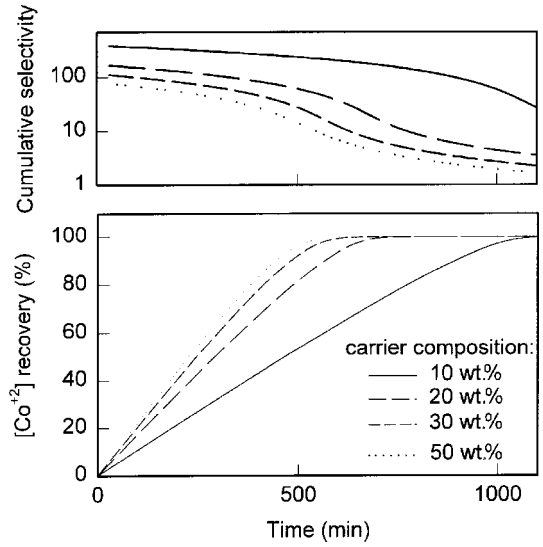

Figure 11. Changes in the recovery of Co and cumulative selectivity with time at various carrier compositions ($[Co^{+2}]_F$, $[Ni^{+2}]_F = 170\,mol/m^3$, $pH_F = 6.0$, feed flow rate = 1000 ml/min, feed and receiving volume = 1000 ml).

concentrations. The concentrations of cobalt and nickel in feed solution were 170 mole/m^3, respectively. The recovery rate of cobalt increases with time and carrier concentration while the selectivity decreases. The increase in the carrier concentration can reduce the operation time for recovering cobalt at the cost of selectivity. The separation of cobalt took about 1000 min for a complete recovery at the carrier concentrations of 10 wt.%. The selectivity for this case is 40 and the purity of cobalt in the strip solution is 97.8%. When the operation time was reduced to 900 min the recovery rate was about 90% while the selectivity was 100, suggesting that 99% pure cobalt can be obtained. The requirement for the recovery rate and the purity varies according to individual processes and Fig. 11 can be used as a guideline to select the optimum operation conditions for each process.

CONCLUSIONS

A mathematical model has been developed to analyze the permeation rates and the separation factor of cobalt and nickel across a hollow-fiber

supported liquid membrane containing HEH (EHP) as a carrier and tested using experimental data. The effects of experimental parameters on the permeation characteristic of cobalt was in good agreement with the model prediction. At concentration higher than 0.01 mole/m^3, the permeation rate of cobalt increases sharply with the decrease of the hydrogen ion. However, when the hydrogen concentration decreases below 0.01 mole/m^3, the permeation rate is limited and the effect of the hydrogen was negligible. The permeation rate increases with carrier concentration, showing a maximum at 50–60 wt.% of the carrier concentration and decreases afterwards. High carrier concentration retards the diffusion of cobalt in liquid membrane due to the increase of viscosity and, consequently, reduces the permeation rate. The permeation rate of cobalt is determined by the mass-transfer coefficient in the liquid membrane at higher flow rate where the mass-transfer coefficient in the feed solution is much higher than that in the liquid membrane. The recovery rate of cobalt increases with time and carrier concentration while the selectivity decreases. The increase in the carrier concentration can reduce the operation time for recovering cobalt at the cost of selectivity.

The overall transport characteristics of cobalt and nickel through hollow-fiber supported liquid membrane were understood and extended to the commercial scale. It is expected that the model could be applied to the separation of other metal ions by changing a few parameters such as diffusion coefficient and equilibrium constant, depending on the carrier and metals of interest.

NOMENCLATURE

C	concentration (mole/m^3)
$[CoR_2\ (HR)_2]$	cobalt–carrier complex concentration (mole/m^3)
D	diffusion coefficient (m^2/s)
De	effective diffusivity in liquid-membrane phase (m^2/s)
De_{Co}	De of Co–Carrier complex (m^2/s)
De_{Ni}	De of Ni–Carrier complex (m^2/s)
$[(HR)_2]$	concentration of carrier (mole/m^3)
J	permeation rate (mole/m^2 s)
Ke	extraction equilibrium constant (—)
k	mass-transfer coefficient in aqueous boundary layer (m/s)
$[NiR_2\ (HR)_4]$	nickel–carrier complex concentration (mole/m^3)
r^2	coefficient of determination (—)
S	shape factor (—)
V, v	velocity (m/s)

Greek letters

δ	membrane thickness, = r2 − r1(m)

Superscripts

—	species in organic phase

Subscripts

Co	cobalt
F	feed phase
H	hydrogen
i	interface
in	initial
Ni	nickel
S	strip phase

REFERENCES

1. Teramoto, M.; Tanimoto, H. Mechanism of copper permeation through hollow fiber liquid membranes. Sep. Sci. Technol. **1983**, *18* (10), 871–892.
2. Danesi, P.R. A simplified model for the coupled transport of metal ions through hollow-fiber supported liquid membranes. J. Membr. Sci. **1984**, *20*, 231–248.
3. de Haan, A.B.; Bartels, P.V.; de Graauw, J. Extraction of metal ions from waste water. Modeling of the mass transfer in a supported-liquid-membrane process. J. Membr. Sci. **1989**, *45*, 281–297.
4. Kim, J.-I.; Stroeve, P. Uphill transport in mass separation devices with reactive membranes: counter-transport. Chem. Eng. Sci. **1989**, *44* (5), 1101–1111.
5. Urtiaga, A.M.; Irabien, J.A. Internal mass transfer in hollow fiber supported liquid membranes. AIChE J. **1993**, *39* (3), 521–525.
6. Jensen, V.G.; Jeffrey, G.V. Numerical methods. *Mathematical Methods in Chemical Engineering*, 2nd Ed.; Academic Press: New York, 1977; 413.
7. Ibanez, J.A.; Victoria, L.; Hernandez, A. Flux and characteristic parameter in mediated transport through liquid membrane 1. A theoretical model. Sep. Sci. Technol. **1989**, *24* (1&2), 157–164.
8. Juang, R.-S.; Jiang, J.-D. Rate-controlling mechanism of cobalt transport through supported liquid membranes containing di(2-ethylhexyl)-phosphoric acid. Sep. Sci. Technol. **1994**, *29* (2), 223–237.
9. Bennett, C.O.; Myers, J.E. Fluid dynamics. *Momentum, Heat and Mass Transfer*, 2nd Ed.; McGraw-Hill, Inc.: New York, 1974; 144.

10. Bird, R.B.; Stewart, W.E.; Lightfoot, E.N. *Transport Phenomena*; John Wiley & Sons, Inc.: New York, 1960; 47.
11. Kim, J.-I.; Stroeve, P. Uphill transport of dilute solute in mass separation devices with reactive co-transport membranes. J. Membr. Sci. **1990**, *49*, 37–53.
12. Komasawa, I.; Otake, T.; Hattori, I. Extraction of nickel and cobalt with 2-ethylhexyl-phosphonic acid mono-2-ethylhexyl ester. J. Chem. Eng. Jpn. **1983**, *16*, 210.
13. Preston, J.S. Solvent extraction of cobalt and nickel by organophosphorus acids: 1. Comparison of phosphoric, phosphonic acid systems. Hydrometallurgy **1982**, *9* (2), 115.
14. Neuman, R.D.; Zhou, N.F.; Wu, J.; Jones, M.A.; Gaonkar, A.G.; Park, S.J.; Agrawal, M.L. General model for aggregation of metal–extractant complexes in acidic organophosphorus solvent extraction system. Sep. Sci. Technol. **1990**, *25* (13–15), 1655–1674.
15. Bennett, C.O.; Myers, J.E. *Momentum, Heat and Mass Transfer*, 2nd Ed.; McGraw Hill, Inc.: New York, 1974; 24.
16. Skelland, A.H.P. Molecular diffusivities. *Diffusional Mass Transfer*; John Wiley & Sons: New York, 1974; 54–77.
17. Danesi, P.R.; Reichley-Yinger, L.; Cianetti, C.; Rickert, P.G. Separation of cobalt and nickel by liquid–liquid extraction and supported liquid membranes with (2,4,4-trimethylpentyl) phosphinic acid (CYNEX 272). Solvent Extr. Ion Exch. **1984**, *2* (6), 781–814.
18. Weast, R.C. Ed. *CRC Handbook of Chemistry and Physic*, 65th Ed.; CRC press: Boca Raton, 1985; D-171.
19. Reid, R.C.; Prausnitz, J.M.; Poling, B.E. *The Properties of Gases & Liquids*, 4th Ed.; McGraw-Hill: N.Y., 1987; 620–623.
20. Green, D.W., Ed. *Perry's Chemical Engineers' Handbook*, 6th Ed.; McGraw-Hill: NY, 1984; 3–287.
21. Youn, I.J.; Lee, Y.; Lee, W.H. Analysis of permeation rate of cobalt ions across a supported liquid membrane containing HEH(EHP). J. Membr. Sci. **1995**, *100*, 69–75.
22. Lee, J.-C.; Jeong, J.; Youn, I.J.; Chung, H.-S. Selective and simultaneous extractions of Zn and Cu ions by hollow fiber SLM modules containing HEH(EHP) and LIX84. Sep. Sci. Technol. **1999**, *34* (8), 1689–1701.
23. Youn, I.J.; Lee, Y.; Jeong, J.; Lee, W.H. Analysis of Co–Ni separation by a supported liquid membrane containing HEH(EHP). J. Membr. Sci. **1997**, *125*, 231–236.

Received January 2002
Revised July 2002